The Era of Multi-Messenger Solar Physics
Proceedings IAU Symposium No. 372, 2023
G. Cauzzi & A. Tritschler, eds.
doi:10.1017/S1743921322004744

Spectroscopic Detection of Alfvénic MHD Waves in the Sunspot Chromosphere

Jongchul Chae

Seoul National University, Seoul, Korea

Abstract. Alfvénic waves are regarded as an important process in understanding coronal heating, solar wind acceleration, and the fractionization of low first-ionization-potential (FIP) elements. Recently, significant progresses have been made in the detection of propagating Alfvénic waves in the solar chromosphere using two different methods: the imaging method and the spectroscopic method. The imaging method detects Alfvénic waves that oscillate in the direction perpendicular to the line of sight, and the spectroscopic method, those that oscillates in the line of sight direction. We have applied the spectroscopic method to the imaging spectral data taken by the FISS on GST at Big Bear. As a result, we detected a number of propagating Alfvénic wave packets, and found that there are two distinct groups: three-minute period waves, and ten-minute period waves.

Keywords. line: profiles, MHD, waves, techniques: spectroscopic, Sun: atmospheric motions, Sun: chromosphere, Sun: oscillations, sunspots

1. Introduction

Alfvénic MHD waves refer to transverse MHD waves that propagate along magnetic field lines. They include pure Alfvén waves, either shear Alfvén waves in a planar geometry or torsional Alfvén waves in a magnetic flux tube, that are fully incompressive, and kink waves in a magnetic flux tube, that are weakly compressive. Even though pure Alfvén waves and kink waves differ in their physical nature (Van Doorsselaere et al. 2008), they are similar to each other in that both are transverse and both propagate along magnetic field lines. Moreover, they can be mutually converted under some conditions (Cranmer & van Ballegooijen 2005), which justifies the use of the term Alfvénic waves without having to discern between the two kinds.

Alfvénic waves have been theoretically investigated for long time because they are considered important in the solar research. As they are an efficient carrier of energy, they are believed important in the problem of coronal heating (Alfvén 1947; Osterbrock 1961). In addition, Alfvénic waves produce the pondermotive force that can drive charged particles along magnetic field lines (Litwin & Rosner 1998), so they may hold keys to understanding the problem of solar wind acceleration (Cranmer & van Ballegooijen 2005), and the problem coronal abundance enhancement of low FIP elements (Laming 2004).

The detection of Alfvénic waves has been mostly done with the imaging method. In this method, transverse kink motions on the plane of sky are inferred from the time variation of the shape of chromospheric threads. This method was successfully used to detect Alfvénic waves in the limb spicules (De Pontieu et al. 2007), and disk fibrils either in active regions (He et al. 2009; Pietarila et al. 2011) or in quiet regions (Jess et al. 2012). It was also shown with this method that Alfvénic waves pervade in sunspot superpenumbral fibrils (Morton et al. 2021).

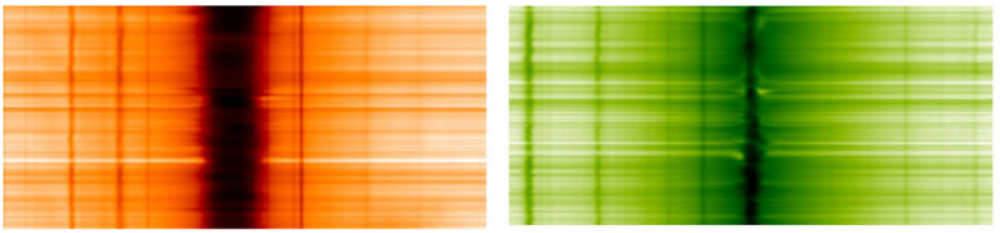

Figure 1. Example of the Hα spectrogram (left) and the Ca II 8542 spectrogram (right) simultaneously taken by the FISS.

The spectroscopic detection of Alfvénic waves in the chromosphere has been very rare. A very earlier attempt to determine the line-of-sight velocity oscillations associated with Alfvénic waves in chromospheric fibrils was made by Giovanelli (1975) based on the spectral scan of the Hα line using a tunable narrowband birefringent filter. As far as we know, we are the first who clearly detected Alfvénic waves in chromospheric fibrils with a real spectrograph. In this proceeding, we will briefly review the spectroscopic data and method we have used, and the main findings we have obtained (Chae et al. 2021b, 2022).

2. Data and Method

To obtain the spectral data, we used the Fast Imaging Solar Spectrograph (FISS) on the 1.6 meter Goode Solar Telescope at the Big Bear Solar Observatory. The FISS is a dual-band Echelle Spectrograph with the imaging capability based on the raster scan of the slit over the field of view (Chae et al. 2013). By default, it simultaneously records the spectrogram around the Hα line by camera A and the spectrogram around the Ca II 8542 line by camera B (see Fig 1). The spectral resolving power is higher than 10^5 in both bands. The raster scan of a $20''$-width field of view is typically done every 20 s. The spatial resolution depends on the seeing and the performance of the instrument, and can be as high as $0.''32$.

The physical parameters are inferred from each line profile taken at a point at a specific instant based on spectral inversion. For this purpose, we have developed the technique of multilayer spectral inversion (MLSI, Chae et al. 2020, 2021a). In this technique, the atmospheric consists of three layers: the photosphere, the lower chromosphere, and the upper chromosphere. The radiative transfer in each layer is described by the parameters: source function, Doppler width, and line-of-sight velocity, with their height variations being described by the first polynomials of optical depth. The model has ten free parameters, seven among which are the parameters of the chromospheric layers. The left panel of Fig. 2 illustrates the MLSI fitting of the Hα line profile.

The most useful parameters are the line-of-sight velocity, the Doppler width, and the source function at the upper layer where the line core is formed. Particularly the line-of-sight velocity data is used to detect velocity oscillations along the line of sight. Once the inversion is done at every point inside the field of view, one can construct the map of line-of-sight velocity as shown in the right panel of Fig. 2. The time series of spatially aligned velocity maps allows us to investigate the velocity oscillation at an arbitrary point inside the field of view.

The principle of spectroscopic Alfvénic wave detection is rather simple. We choose chromospheric features like fibrils that are highly elongated in the plane of sky. In a feature of this kind, magnetic field lines are likely to be quite along the direction of elongation direction, and to be very much perpendicular to the line of sight. Then, as illustrated in Fig. 3, the oscillations of line-of-sight velocity at a point on the feature

https://doi.org/10.1017/S1743921322004744 Published online by Cambridge University Press

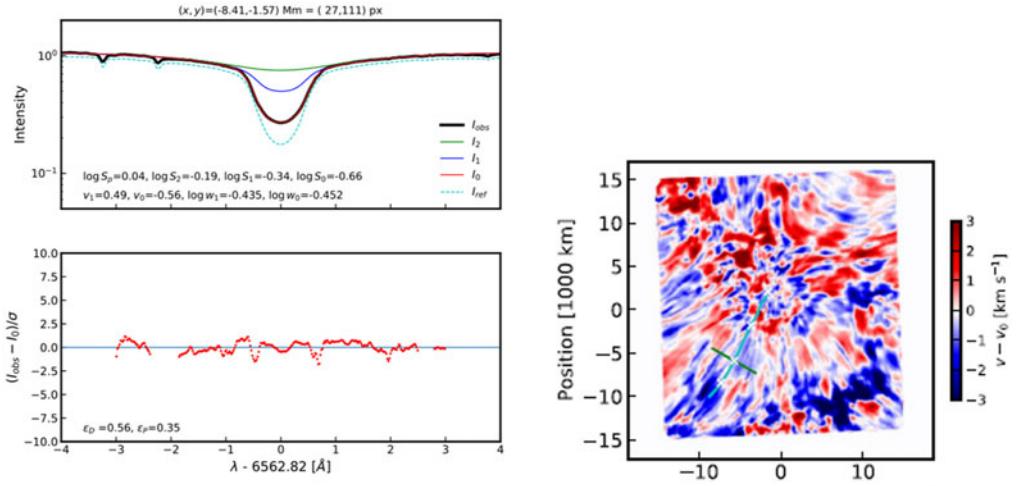

Figure 2. Example of the MLSI fitting of the Hα line profile (left) and the map of the line-of-sight velocity inferred from the Hα line inversion (right).

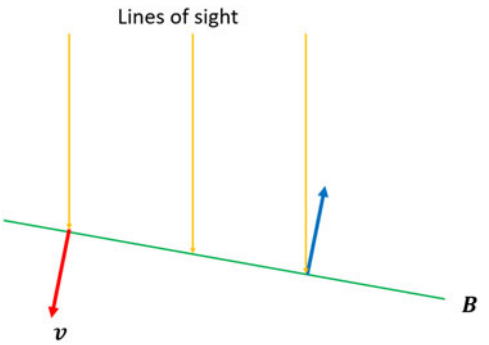

Figure 3. Illustration of spectroscopic Alfvén wave detection.

is mostly attributed to the oscillations of transverse velocity across the field lines. The analysis of these oscillations will yield the value of velocity amplitude as well as wave period. Moreover, if the velocity oscillations at two points that are located apart in the same feature are correlated with each other with a finite time lag, one can determine the direction and speed of wave propagation along the feature, which is expected to be comparable to the Alfvén speed in the chromosphere.

Our data provide us with another test for the verification of Alfvén waves. Since Alfvén waves are either incompressive or weakly compressive, the velocity oscillations will not accompany the oscillations of pressure and temperature. Temperature can be determined from the Doppler width of the Hα line. We can check whether velocity oscillations and temperature oscillations are strongly correlated with each other or not.

3. Results

The first spectroscopic detection of Alfvénic waves in the chromosphere was done by Chae et al. (2021b) in numerous fibrils around a small sunspot. The Hα intensity map of the observed region is shown in the upper left of Fig. 4. Point A corresponds to the center of this sunspot. As illustrated in the upper right of the figure, the line of sight at this point is almost parallel to the magnetic field lines, so the line-of-sight

https://doi.org/10.1017/S1743921322004744 Published online by Cambridge University Press

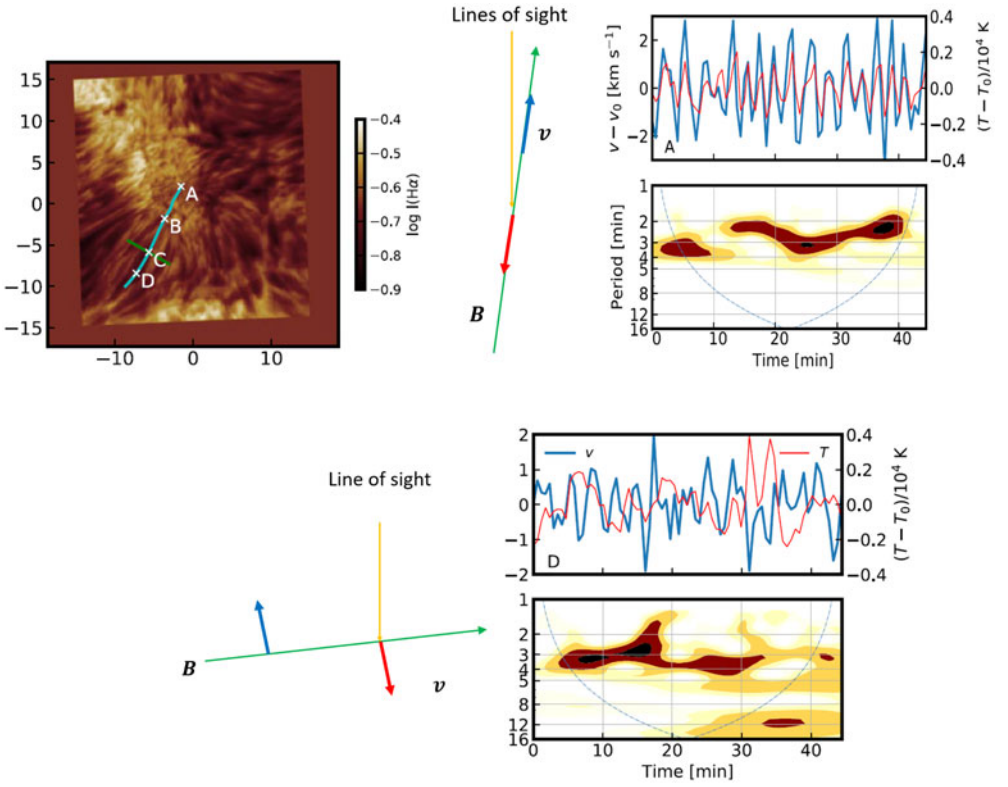

Figure 4. Points of interest marked on the map of Hα core intensity (upper left), the oscillations of velocity and temperature at point A (upper right), and those at point D (lower).

velocity oscillations represent the longitudinal velocity oscillations. These are the well-known umbral oscillations of velocity that are interpreted as slow MHD waves under the influence of gravity. At this point A, the temperature fluctuations well correlated with the velocity oscillations, which is consistent with the compressive nature of the waves.

Point D is located on a fibril emanating from the sunspot. At this point, magnetic field lines are predominantly perpendicular to the line of sight as depicted at the bottom of Fig. 4. Therefore, the velocity oscillations measured at this point shown at the bottom of Fig. 4. are likely to represent mostly the transverse oscillations of velocity. The figure also presents the temperature fluctuations at D, which are not correlated with the velocity oscillations at all, suggesting the incompressive nature of the velocity oscillations. The time-distance map of velocity constructed along the fibril (shown in Chae et al. 2021b) indicates that these velocity oscillations propagate at speeds around 100 km s^{-1}. Therefore, the velocity oscillations at D may be attributed to Alfvénic waves in the chromospheric fibril.

It was later realized by Chae et al. (2022) that the detection of Alfvénic waves of different periods can be done more systematically by decomposing the velocity fluctuations into a few band-filtered oscillations. Fig. 5 presents some maps of band-filtered velocity as well as that of the non-filtered velocity. The map of velocity with periods from 3.0 to 7.0 min reveals red-colored (i.e. redshifted) velocity stripes that are radially extended, much more clearly than the map of non-filtered velocity. The velocity stripes of this kind is a signature of the presence of Alfvénic waves because Alfvénic waves have a high speed of propagation and a very long wavelength. The value of propagation speed

https://doi.org/10.1017/S1743921322004744 Published online by Cambridge University Press

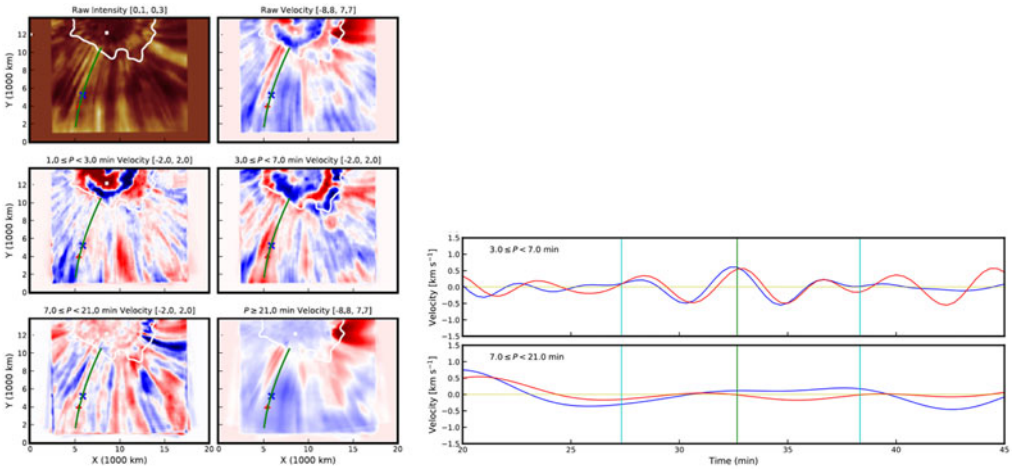

Figure 5. Maps of Hα core intensity, non-filtered line-of-sight velocity, and band-filtered velocities (left), and illustration of the cross-correlation analysis of band-filtered velocity oscillations at two points (right).

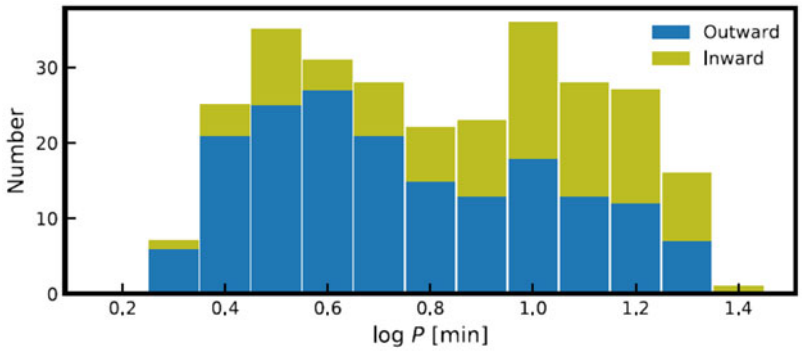

Figure 6. Number distribution of wave period indicating two groups of waves: three-minute waves and ten-minute waves.

can be determined by the analysis of cross correlation between the band-filtered velocity oscillations at two points as illustrated at the right of Fig. 5. In this specific case, the propagation speed was found to be 80 km s^{-1}.

We detected Alfvénic waves 279 times at different locations and at different times. From each detection, we determined the values of period, velocity amplitude, and propagation speed as well as propagation direction. The most interesting is the number distribution of wave period as shown in Fig. 6. The Alfvénic waves we detected can be divided into two groups depending on the period: the group of waves (three-minute waves) with periods around $10^{0.5}$ min and another (ten-minute waves) with periods around $10^{1.0}$ min. The figure also indicates that the three-minutes waves propagate mostly outward from the sunspot, but the ten-minute waves propagate either outward from or inward to the sunspot with roughly equal occurrence rates. Summarized in Table 1 are the typical values of period, propagation speed, and velocity amplitude in the two groups of waves.

4. Summary and Conclusion

From the imaging spectrograph data taken with the FISS on the GST at the Big Bear Solar Observatory, we have successfully constructed the time series of line-of-sight

https://doi.org/10.1017/S1743921322004744 Published online by Cambridge University Press

Table 1. Typical values of observed parameters in three-minute waves and ten-minute waves.

Parameter	Three-minute waves	Ten-minute waves
Period	3.7 min	12 min
Propagation speed	140 km s^{-1}	65 km s^{-1}
Velocity amplitude	0.7 km s^{-1}	0.6 km s^{-1}

velocity maps. Using these velocity data, we successfully detected Alfvénic waves in the chromospheric fibrils surrounding sunspots that oscillate in the vertical direction. The absence of intensity-velocity correlation and the values of determined propagation speeds comparable to Alfvén speeds in the chromosphere strongly support the detection of Alfvénic waves. Our results also strongly suggest that there are two types of Alfvénic waves: three-minute waves and ten-minute waves.

Our study opens the door to the further spectroscopic investigation of Alfvénic waves in the solar chromosphere, not only on sunspot regions, but also in plage regions and quiet regions. It also raises a number of questions that have to be resolved in the future. From the theoretician's point of view, what are the origin of three-minute waves? Is the slow-to-Alfvénic mode conversion we proposed (Chae et al. 2021b) really operating or not? How about ten-minute wave? Are they related to the cutoff period of Alfvénic wave as we proposed (Chae et al. 2022) or not? Do the Alfvénic wave detected with the spectroscopic method much overlap those detected with the imaging method or do they represent distinct kinds of Alvénic waves? From the observer's point of view, is there any way of cleanly separating between compressive slow waves and incompressive Alfvénic waves in penumbral regions as it is likely that these two kinds exist together. If possible, the study of sunspot waves will be very fruitful.

Acknowledgements

This research was supported by the National Research Foundation of Korea (NRF-2020R1A2C2004616 and NRF-2020R1I1A1A01068789). The GST operation is partly supported by the Korea Astronomy and Space Science Institute, the Seoul National University, and the Key Laboratory of Solar Activities of Chinese Academy of Sciences (CAS) and the Operation, Maintenance and Upgrading Fund of CAS for Astronomical Telescopes and Facility Instruments.

References

Alfvén, H. 1947, MNRAS, 107, 211
Chae, J., Cho, K., Kang, J., et al. 2021a, Journal of Korean Astronomical Society, 54, 139
Chae, J., Cho, K., Lim, E.-K., & Kang, J. 2022, ApJ, 933, 108
Chae, J., Cho, K., Nakariakov, V. M., Cho, K.-S., & Kwon, R.-Y. 2021b, ApJ Letters, 914, L16
Chae, J., Madjarska, M. S., Kwak, H., & Cho, K. 2020, A&A, 640, A45
Chae, J., Park, H.-M., Ahn, K., et al. 2013, Solar Phys., 288, 1
Cranmer, S. R. & van Ballegooijen, A. A. 2005, ApJ Suppl., 156, 265
De Pontieu, B., McIntosh, S. W., Carlsson, M., et al. 2007, Science, 318, 1574
Giovanelli, R. 1975, Solar Phys., 44, 299
He, J. S., Tu, C. Y., Marsch, E., et al. 2009, A&A, 497, 525
Jess, D. B., Pascoe, D. J., Christian, D. J., et al. 2012, ApJ Letters, 744, L5
Laming, J. M. 2004, ApJ, 614, 1063
Litwin, C. & Rosner, R. 1998, ApJ Letters, 506, L143
Morton, R. J., Mooroogen, K., & Henriques, V. M. J. 2021, Philosophical Transactions of the Royal Society of London Series A, 379, 20200183
Osterbrock, D. E. 1961, ApJ, 134, 347
Pietarila, A., Aznar Cuadrado, R., Hirzberger, J., & Solanki, S. K. 2011, ApJ, 739, 92
Van Doorsselaere, T., Nakariakov, V. M., & Verwichte, E. 2008, ApJ Letters, 676, L73

https://doi.org/10.1017/S1743921322004744 Published online by Cambridge University Press